

Capstone: Power-Capped Pipelining for Coarse-Grained Reconfigurable Array Compilers

Sabrina Yarzada and Christopher Torng

Department of Electrical and Computer Engineering, University of Southern California, Los Angeles, CA

Abstract—Coarse-grained reconfigurable arrays (CGRAs) have attracted growing interest because they exhibit performance and energy efficiency competitive with ASICs while maintaining flexibility similar to FPGAs. These properties make CGRAs attractive in accelerator and other power-constrained system contexts. However, modern CGRA compilers aggressively pipeline for frequency and performance improvements, often violating hard power budgets. We empirically show that, in state-of-the-art CGRA compilers such as Cascade, post-place-and-route (post-PnR) pipelining increases power monotonically and ultimately exceeds fixed power caps across diverse workloads. In response, we introduce *Capstone*, a power-aware extension of Cascade that integrates a fast, compiler-resident power model with a user-tunable controller that guides the bitstream selection process towards optimization targets. Capstone predicts per-iteration power directly inside the post-PnR compilation loop and selects one or a small set of PnR configurations such that at least one meets a user-specified power cap. Thus, we shift the objective from indiscriminately maximizing frequency to maximizing safe frequency under a discrete power cap. On a suite of kernels spanning fundamental dense and sparse applications, Capstone meets a power cap and minimizes remaining power headroom while preserving feasible performance. Our results indicate that cap-aware compilation is both necessary and practical, as the compiler can proactively land on cap-compliant points and expose predictable performance under power constraints.

I. INTRODUCTION

Reconfigurable spatial computing is a well-studied field in computer architecture, but we call attention to two specific and recent modern parallel trends. First, coarse-grained reconfigurable arrays (CGRAs) have emerged as a compelling architectural middle ground between ASICs and FPGAs [15, 18, 19, 23, 25, 27, 28, 35, 54, 69, 70]. They combine the flexibility of spatial programming with the performance and efficiency of custom accelerators, making them well-suited for rapidly evolving workloads such as neural network inference, image processing pipelines, and sensor fusion. Second, these same workloads are increasingly deployed in power-limited environments such as edge inference, mobile augmented reality, battery-operated camera pipelines, or thermally constrained SoCs. In such domains, exceeding the power budget can lead to throttling or failure, and underutilizing it wastes valuable headroom that could otherwise be traded for speed.

Despite this growing emphasis on efficiency, most modern CGRA compilers optimize only for performance. Prior CGRA compiler flows typically achieve high-frequency operation through conventional scheduling and placement strate-

gies. Cascade [48] introduced a novel form of automated *post-place-and-route (post-PnR) pipelining* that inserts configurable registers along routed interconnect and computation paths to shorten critical paths. This technique significantly improves achievable clock frequency and energy–delay product (EDP), but it also increases switching activity and static power consumption through additional registers and control overhead. As pipeline depth grows, total power rises monotonically, eventually exceeding realistic system caps. In power-limited domains, a compiler that simply “maximizes frequency” risks producing infeasible bitstreams.

Thus, an approach to power capping is necessary to ensure correct system operation and reliability. The key challenge with CGRA power capping lies in the backend compiler’s visibility and control. Cascade [48] performs iterative post-PnR pipelining purely under the guidance of static timing analysis (STA), with no way to observe how each iteration affects power. Our empirical characterization shows that across diverse dense and sparse kernels, each pipelining iteration increases power monotonically until the design exceeds realistic system power caps. Figure 1 illustrates this trend: even modest additions of interconnect registers and frequency increases can push total power well above the cap, with the compiler lacking the awareness to detect or prevent violations. Existing power-capping mechanisms such as runtime DVFS controllers [4, 12, 30, 55, 62, 73, 86, 87] operate only reactively after deployment, and therefore cannot undo structural over-pipelining built into the bitstream. Thus, compile-time decisions themselves must become power-aware to ensure power cap compliance without compromising performance.

Our key insight is that CGRA compilers expose rich structural information describing the architectural datapath, such as the number of active tiles, routing density, and interconnect utilization. This data can be leveraged to estimate power quickly enough for inner-loop decisions, such as in the post-PnR pipelining loop introduced by Cascade [48]. Instead of invoking commercial ASIC sign-off tools that require full parasitic extraction and simulation bottlenecked by run time, the compiler can learn a lightweight model that predicts post-PnR power from its own intermediate representations. By embedding such a model directly into the post-PnR pipelining loop, the compiler can treat power as a first-class optimization objective alongside timing. This perspective shifts

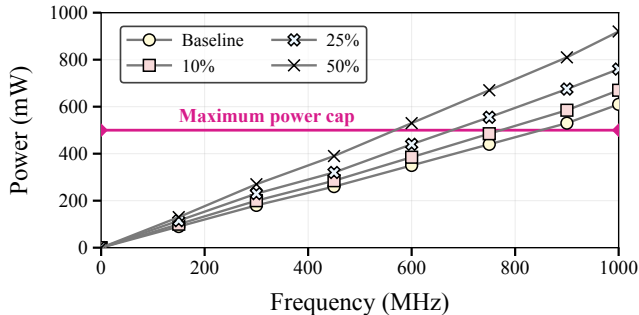


Figure 1. As state-of-the-art CGRA compilers pipeline for higher clock frequencies, they can unknowingly exceed a power cap (horizontal line). For the vector elementwise addition kernel, projections of future incremental performance optimizations (e.g., 10%) for the Cascade compiler all similarly exceed the power cap.

the goal from exclusively maximizing frequency to maximizing safe frequency under a power cap.

Building on this observation, we present Capstone, a power cap-aware extension of Cascade [48]. Capstone integrates a fast, compiler-resident power model calibrated to commercial ASIC sign-off data with a user-tunable controller that guides post-PnR pipelining towards cap-compliant points. During each iteration, the compiler predicts per-configuration power and selects one or a small set of PnR configurations such that at least one satisfies a user-specified power cap at runtime. The controller can operate in multiple modes depending on the desired reliability and run time. This approach allows Capstone to proactively land on near-cap operating points, minimize wasted power headroom, and avoid costly over-pipelined bitstreams.

Our contributions are as follows:

- We develop a hierarchical, machine-learned energy model, trained using gate-level power estimation supervision. The model jointly learns (i) compiler-visible energy events, (ii) their per-event energy costs, and (iii) a mapping to fine-grained RTL power instances, bridging architectural and physical representations to enable accurate, compile-time power estimation without dynamic simulation.
- We design power-aware compiler controllers that explicitly account for model uncertainty and provide reliability-bounded guarantees, ensuring at least one selected bitstream satisfies a user-defined power cap while maximizing achievable frequency.
- We evaluate Capstone across fundamental dense and sparse CGRA kernels, demonstrating accurate compiler-level power prediction, cap compliance, and minimal performance loss relative to unconstrained compilation.

Section II reviews prior work and foundational background on CGRA architectures, compilation, and power estimation,

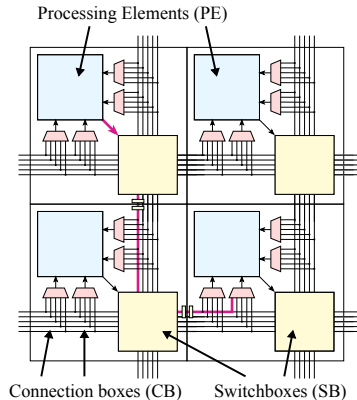


Figure 2. CGRA architecture including PE tiles and interconnect components (SBs, CBs). The pink route highlights a representative routed critical path that post-PnR pipelining breaks by inserting green registers along the interconnect. Input and output tracks along the north and west perimeters are connected to memory banks.

motivating the need for cap-aware compilers. Section III details the design of Capstone’s compiler-level energy model and its controller mechanisms. Section IV presents our experimental results and comparisons against state-of-the-art CGRA compilers. Our results indicate that cap-aware compilation is both necessary and practical as the compiler can proactively land on cap-compliant points and expose predictable performance under power constraints.

II. BACKGROUND AND RELATED WORK

Coarse-grained reconfigurable arrays (CGRAs) [15, 18, 19, 23, 25, 27, 28, 35, 54, 69, 70] are a class of programmable accelerators that combine architectural flexibility with improved performance and energy efficiency compared to fine-grained architectures such as FPGAs [14, 63]. As illustrated in Figure 2, a representative CGRA from [35] is composed of an array of processing element (PE) tiles, memory (MEM) tiles, and I/O tiles interconnected via a reconfigurable routing interconnect with configurable pipelining registers. These tiles work together to execute operations such as additions, multiplications, and memory accesses in a statically scheduled dataflow graph.

Pipelining is essential for high-throughput CGRAs, whose long interconnects and compute chains limit clock frequency. Cascade [48] introduced a post-PnR pipelining technique that iteratively inserts registers along critical paths using configurable interconnects and STA feedback. While this improves maximum frequency and EDP, it follows a performance-first policy, ignoring the power and energy overheads of deeper pipelining where each stage adds dynamic switching and static costs. As shown in Figure 3, power rises monotonically with pipeline depth. Because many CGRA deployments operate under strict thermal or battery power budgets [1, 33, 34], compilers should optimize performance *within* a power cap rather than pursuing unconstrained frequency. However, existing CGRA compilers [17, 21, 32, 46, 47, 78, 81, 83], including Cascade [48], are *power-unaware*. They pipeline aggressively without estimating or constraining power. This limitation motivates Capstone, a cap-guided compiler that integrates fast energy modeling into Cascade’s post-PnR loop.

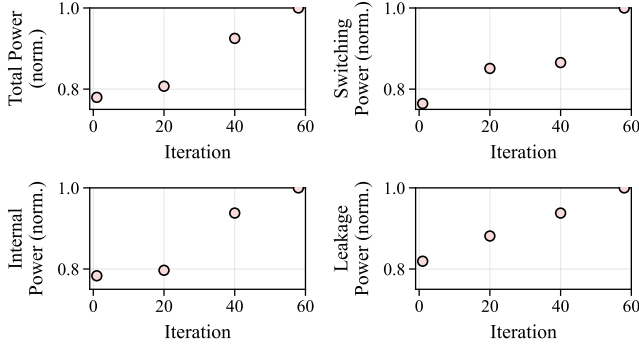


Figure 3. Normalized power vs post-PnR pipelining iteration for the vector elementwise addition kernel used by Cascade [48].

Power can be estimated at several stages of the ASIC flow [7, 29, 75], trading fidelity for speed. Gate-level sign-off with post-PnR parasitics is most accurate but much too slow for iterative compilation. Analytical frameworks like McPAT [42] are faster but neglect domain-specific component costs that dominate CGRA power. Compiler-time estimators must therefore be both fast and sufficiently accurate. Common approaches include (i) analytical models mapping activity events to both dynamic energy and leakage terms, and (ii) learning-based estimators [36, 37, 39, 43, 52, 59, 71, 80, 84]. Capstone adopts a learning-based approach in building a compiler-resident, gate-level-supervised energy model that systematically and incrementally approaches more detailed and accurate energy costs.

Compiler-level power models inevitably diverge from post-layout estimates because they compress detailed bit-level switching and parasitic effects into a small set of lumped events, and successive pipelining iterations in CGRA backends such as Cascade further perturb routing and effective capacitance. Figure 4 shows the percentage error between gate-level, signoff power estimates from commercial ASIC tools and one manually calibrated instance of Capstone’s model, indicating that while distilled models can recover the correct order of magnitude, meaningful error is unavoidable. Accordingly, Capstone accounts for estimation uncertainty rather than assuming a single-point oracular model, using probabilistic guarantees inspired by robust and chance-constrained optimization [5, 6, 10, 13, 16, 26, 38, 51, 53, 57, 58, 61, 64, 66, 76, 79] to ensure runtime power-cap compliance while maximizing frequency and bounding violation risk.

Beyond CGRAs, energy-aware compilation and power control have been studied across CPUs, GPUs, and accelerators [44, 49, 50, 68, 74]. Post-PnR frameworks such as Simmani [30], NeuroMeter [67], and PowerProbe [85] provide accurate estimation but are too slow for inner compiler loops, while run-time controllers [4, 86, 87] rely on reactive feedback rather than structural prevention. Capstone complements these efforts by ensuring run-time power cap compliance, producing bitstreams that already operate near the target cap without the need for reactive fixes such as post-

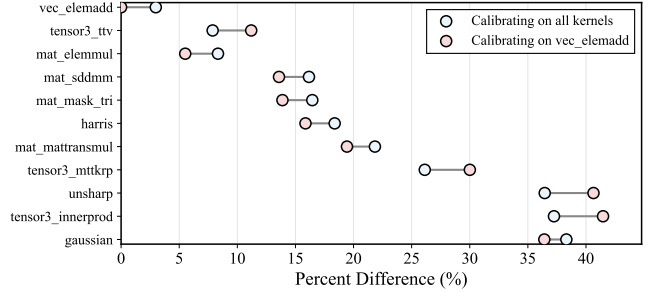


Figure 4. PTPX vs Capstone model power estimates comparison. Red calibrates on only `vec_elemadd`; blue calibrates on all kernels.

deployment throttling. Furthermore, theoretical foundations from robust optimization, distributionally robust optimization (DRO) [3, 41, 72, 82], and conformal prediction [8, 9, 20, 45, 77] inform Capstone’s power-aware controllers.

In summary, prior work spans energy-aware compilation, post-PnR modeling, run-time control, and uncertainty-aware optimization. However, we find that no prior works support the fast, fine-grained, power-aware decisions needed within a CGRA compiler. Capstone fills this gap by unifying fast energy modeling, uncertainty handling, and compile-time power-capping into one integrated flow.

III. CAPSTONE: POWER-AWARE COMPILATION UNDER CONFIDENCE GUARANTEES

A reasonable approach to quantify a CGRA’s power at compile time without any additional infrastructure is to snapshot the PnR graph at a chosen point within a pipelining pass, then construct the corresponding hardware netlist offline, and then run a sign-off quality power estimation tool. This is the procedure we used to generate the data in Figure 3. While feasible, this method immediately exposes a run time bottleneck. That is, repeatedly invoking sign-off quality power estimation inside the compiler is much too slow (hours) for an inner loop, motivating a fast, predictive model.

Capstone augments Cascade’s post-PnR pipelining loop with (i) a fast compiler-level energy model that runs inline with STA and (ii) a controller that selects a set of K PnR configuration candidate bitstreams such that at least one meets a user-specified power cap with a target confidence level while minimizing the remaining power headroom.

A. Energy Model Learning with Gate-Level Supervision

We develop a data-driven, hierarchical methodology for learning compiler-visible energy models in which signoff-quality gate-level power analysis using tools such as Synopsys PRIMETIME PX (PTPX) supervises the discovery of energy events and their mapping to compiler-level activity features. The key objective is to retain the *physical grounding* of gate-level measurements while delivering a fast *compile-time* estimator suitable for inner-loop optimization. Figure 5 outlines our proposed flow. The compiler and PTPX view

TABLE I. CAPSTONE ENERGY MODEL NOTATION.

Symbol	Description	Symbol	Description
E	# compiler events	R	# PRIMETIME PX rows
k	Dataset index	$X^{(k)}$	Event-count vector
$y^{(k)}$	PRIMETIME PX row power	W	Event→row weights
$W_{:,e}$	Column e of W	α	Energy coefficients
α_e	Coefficient for event e	$\hat{y}^{(k)}$	Predicted row power
$\hat{P}^{(k)}$	Predicted total power	$\mathbf{1}$	All-ones vector
λ_W	ℓ_1 weight on W	λ_α	ℓ_2 weight on α

the *same* execution through different fidelities, and training learns a representation that is faithful to PTPX yet evaluable from compiler-visible features alone. This approach bridges physical and architectural power representations, allowing compile-time power estimation without dynamic simulation. Because the learned coefficients encode energy per event at a fixed operating point, the compiler converts them to power via estimated event rates (events/cycle \times frequency), enabling compile-time power capping. Concretely, $P \approx f \sum_e \alpha_e x_e + P_{\text{leak}}$. We summarize notation in Table I.

Typically, the mapping from compiler-visible features to gate-level power report labels is done manually by humans in the loop, but learning replaces that and makes it automatable. Combining the learned mapping with an automated regression loop to tune the numbers produces an overall automatable approach that generates higher-quality power models over time using only compiler-visible features.

For a given input, schedule, and configuration, the compiler propagates concrete dataflow through an abstract architectural datapath (exposing event/activity counts). Simultaneously, PTPX evaluates the corresponding gate-level datapath with input data, reporting instance-level power, including toggle activity and leakage. We therefore treat the compiler and PTPX as two complementary lenses over one execution trace. Our model reorganizes the PTPX hierarchy into a sum-of-products representation (*event count* \times *event cost*) whose total is tuned to match that reported by PTPX at a fixed operating point. The key idea is to learn a representation that is physically grounded at training time (by aligning with PTPX) yet fully evaluable at compile time (using only compiler-visible features).

For each activity realization k , let $y^{(k)} \in \mathbb{R}_{\geq 0}^R$ be the PTPX per-row power vector (rows from the hierarchical power report that enumerate gate-level instances) and let $X^{(k)} \in \mathbb{R}_{\geq 0}^E$ be the compiler-visible event counts. We learn a nonnegative weight matrix $W \in \mathbb{R}_{\geq 0}^{R \times E}$ that distributes each event across PTPX rows and nonnegative per-event coefficients $\alpha \in \mathbb{R}_{\geq 0}^E$ that scale average per-instance energy by containing per-event energy magnitudes. The columns of matrix W indicate which PTPX rows each event pays attention to. This forms the basis of the row-level predictor $\hat{y}^{(k)}$ and total predicted power $\hat{P}^{(k)}$

$$\hat{y}^{(k)} = W \text{diag}(\alpha) X^{(k)}, \quad \hat{P}^{(k)} = \mathbf{1}^T \hat{y}^{(k)}. \quad (1)$$

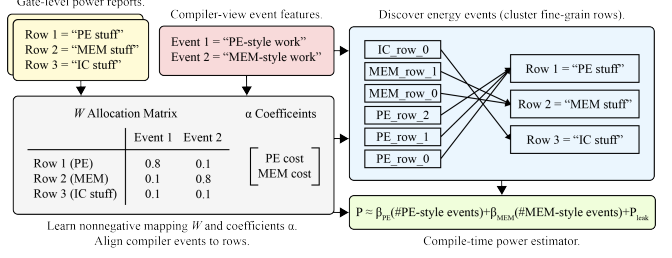


Figure 5. Hierarchical energy model learning. We learn a nonnegative mapping W and per-event coefficients α that align compiler events to gate-level rows, discover energy events from per-row power, then perform compile-time prediction via a sum-of-products over compiler-visible features.

For convenience, we define the effective per-event coefficient β_e , which folds the learned row-allocation (W) into a single compile-time weight. At compile time, prediction \hat{P} reduces to the sum-of-products over compiler-visible events

$$\hat{P}^{(k)} = \mathbf{1}^T \hat{y}^{(k)} = \sum_{e=1}^E \beta_e X_e^{(k)}, \quad \beta_e \triangleq \alpha_e \sum_{r=1}^R W_{re}. \quad (2)$$

Parameters (W, α) are learned to minimize discrepancy with PTPX over many datasets while maintaining physical interpretation via nonnegativity and mild regularization:

$$\min_{W, \alpha \geq 0} \sum_k \|y^{(k)} - \hat{y}^{(k)}\|_2^2 + \lambda_W \|W\|_1 + \lambda_\alpha \|\alpha\|_2^2.$$

Here, λ_W and λ_α are hyperparameters. This setup distributes each event across rows (W) and sets per-event costs (α) to better align the model’s predictions with PTPX estimates. The ℓ_1 regularization causes each event (each column of W) to select a small, meaningful group of rows, making the mapping easier to interpret. The ℓ_2 regularization on α keeps the learned energy values smooth and consistent across datasets. We learn W and α jointly so that $\hat{y}^{(k)}$ matches the measured PTPX vector $y^{(k)}$ across many activity samples. The result is a hierarchical energy model that preserves a physically grounded relation to gate-level power estimates via the learned mapping while remaining lightweight enough for design-space exploration.

We solve this with alternating nonnegative updates. Holding α fixed, each column of W is updated by nonnegative least squares (NNLS) with a small ℓ_1 penalty. Holding W fixed, α is updated by nonnegative ridge regression. Each time we update W , we rescale its columns and transfer that scale into α . This eliminates the redundancy where W and α could be scaled in opposite directions without changing the final model. This procedure has two important properties: (i) it learns which rows matter for each event (the “attention” pattern in W) and (ii) it learns how much each event costs on average (the coefficients α), using supervision provided by the gate-level power hierarchy.

We initialize the model by connecting each compiler-level event to all PTPX rows with uniform weights in W , and by

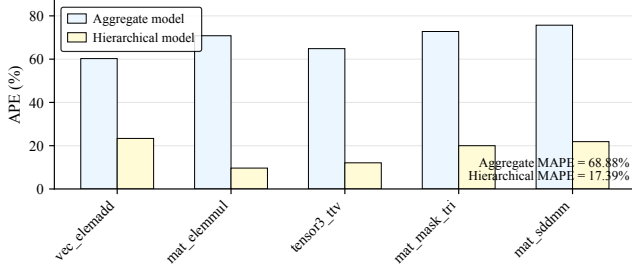


Figure 6. LOOCV total power prediction error (MAPE) for aggregate vs hierarchical energy models across CGRA kernels.

setting α using a simple NNLS fit to total power. The model is then jointly calibrated across all kernels and activity realizations, since the mapping from event space to PTPX rows should remain stable for a fixed design and operating point. During alternating updates, each column of W naturally shifts toward the row groups that consistently co-vary with that event, yielding a fully data-driven, nonnegative mapping. Hyperparameters ($\lambda_W, \lambda_\alpha$) are selected by nested validation, and training uses early stopping when the validation error stops improving. As new datasets arrive, we start from the last learned (W, α) and run a few additional alternating steps, allowing the model to track gradual shifts in the data while preserving its underlying structure.

We train on multiple *activity datasets* (e.g., different input distributions, schedules, or configuration variants) that exercise the same abstract datapath. Each dataset yields a pair $(X^{(k)}, y^{(k)})$. Since the compiler and gate-level power tool capture the same underlying execution at different fidelities, PTPX naturally serves as supervision for learning from compiler-visible events. Inconsistent mappings are penalized by the residual $\|y^{(k)} - \hat{y}^{(k)}\|_2$.

Although the compiler pushes concrete data through the datapath, notable contributions to gate-level power (e.g., fine-grained toggle rates, duty cycles, varying bitwidth across events) are not explicitly available as features at prediction time. Therefore, the learned parameters represent expectations over these hidden factors under the training distribution: α_e is the expected per-instance energy of event e , and W_{re} is the expected allocation of that event’s energy to row r . This marginalization is valid when deployment activity that looks similar to the training activity. The event features capture enough of the datapath structure so that leftover variation averages out across many instances, and the operating conditions $\{V, f, \text{corner}\}$ match those used in training (or are handled with separate parameter sets). This explicitly acknowledges the abstraction gap while allowing the learned model to remain accurate *on average* and robust enough to drive compile-time decisions.

Generalization of the constructed energy model is evaluated and improved iteratively via *leave-one-kernel-out* (LOOCV) insights. That is, in each fold we hold out one kernel (including all of its input/activity variants), train on the

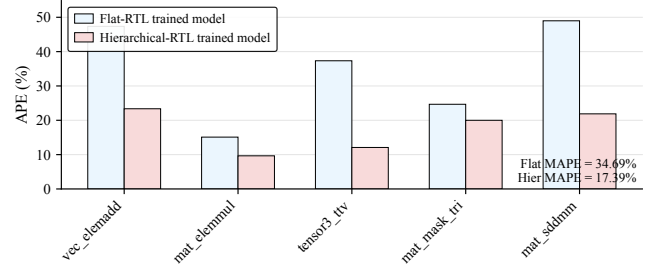


Figure 7. LOOCV total power prediction error (MAPE) for energy models trained on flat vs hierarchical RTL power reports.

remainder, and predict the held-out kernel using the model. This evaluates how well the model transfers across different applications, which reflects real deployment. We report MAPE and R^2 for in-sample fits and LOOCV predictions. For the hierarchical model, we also report the row-level reconstruction error $\|y^{(k)} - \hat{y}^{(k)}\|_2$ and evaluate how stable W is across folds. All evaluations are at matched operating points. When multiple $\{V, f, \text{corner}\}$ exist, a separate energy model is learned per point.

Our hierarchical energy modeling methodology is flexible across different architectures, as it only requires: (i) compiler-visible activity features that are stable across different datapaths, (ii) any post-layout, gate-level power reporter with per-instance breakdown. By learning the mapping from event space to gate-level power report rows jointly over multiple datasets, the model captures a reusable, physically grounded relationship that supports rapid design-space exploration.

We support two learning regimes. The *scalar aggregate* baseline omits W and fits α to totals, $\hat{P}^{(k)} = \sum_e \alpha_e X_e^{(k)}$, via NNLS with a small ridge term. This provides interpretable pJ/event coefficients with guaranteed nonnegativity. In the *hierarchical model*, we use the full PTPX vector $y^{(k)}$ and jointly learn event costs α and weight matrix W that maps events to PTPX rows via alternating updates as described previously. Supervising at the *row* level (fitting the full gate-level hierarchical power report vector instead of only total power) gives the model many more informative constraints. This reduces ambiguity in the learned factors, improves generalization to new kernels, and yields a clear per-row power breakdown consistent with PTPX. Figure 6 shows that this additional structure consistently lowers total power MAPE relative to PTPX estimates across all kernels, tightening Capstone’s power estimates and reducing wasted headroom.

The PTPX reports used for training can be obtained from either a hierarchical RTL netlist or a more flat one. The hierarchical reports group rows by architectural blocks (tiles, interconnect, etc.), which makes the learned columns of W more interpretable and slightly improves accuracy, while flat reports produce a more diffuse allocation. Figure 7 illustrates this tradeoff. Thus, we equip Capstone with a hierarchical, row-supervised energy model trained on hierarchical gate-

TABLE II. CAPSTONE CONTROLLERS NOTATION.

Symbol	Description	Symbol	Description
x	PnR configuration	f	Clock frequency (MHz)
$graph$	PnR graph	Π	Initiation interval
$\hat{P}(x)$	Predicted power (mW)	$P^{true}(x)$	True power
P^{PTPX}	PTPX reference power	μ	$\hat{P}(x)$ shorthand
C	Power cap (mW)	K	# returned bitstreams
γ	Guardband	γ_{anc}	Anchor guardband
γ_{spec}	Speculative guardband	U_{gb}	Guardband upper bound
α	Miscoverage level	$q_{\alpha}(g)$	Conformal residual quantile
U_{conf}	Conformal upper bound	$\rho(f)$	Frequency scaling
\mathcal{D}_{cal}	Calibration set	s_i	One-sided residual
g	Calibration group	$\phi(x)$	Feature vector
λ	Diversity weight	Δf	Min. freq. step
M_i	Error-bounded model	ϵ_k	Event error bound

level power reports, while remaining compatible with flatter RTL styles when needed.

B. Compiler-Level Power-Aware Controllers

In order to consider and limit power during the iterative post-PnR pipelining loop, the integration of a power controller into the compiler is necessary. With quantified power now available from our predictive power model, the controller is responsible for steering the optimization framework as described in Figure 8. That is, given user-defined design knobs including a power cap, confidence target, and the number K of bitstreams to produce, the compiler must return K bitstreams while maximizing performance under the power cap, and ensuring that at least one of the returned bitstreams truly meets the power cap at runtime. We summarize notation in Table II.

As discussed previously, we must embrace the inevitable inaccuracy present in compiler-level power models. We therefore consider two styles of guarantees: *probabilistic* guarantees, which aim to keep the violation probability small but nonzero, and *hard* guarantees, which hold as long as the true model lies within a specified bounded-uncertainty family. Capstone exposes three planner modes within a single compiler-level power controller, selectable by the user based on how much information and calibration effort is available, with more fidelity provided by modes that accept more information. Capstone I describes a Guardband planner that relies on a conservative static safety margin to approximate our three optimization targets (Figure 8) with a confidence dictated by a multiplicative margin. This is the simplest planner, requiring no calibration data, but is also the least capable of simultaneously optimizing all targets. Capstone II introduces a conformal-envelope planner governed by a learned safety margin, providing a finite-sample, distribution-free guarantee of a safe bitstream with confidence of at least $1 - \alpha$ for small α , at the cost of a calibration dataset. Finally, Capstone III provides a hard guarantee by requiring the user to manually specify a set of bounded error ranges on the energy model. Within these bounds, the controller exhaustively reasons about worst-case model error.

Capstone I: Guardband Planner (Static Safety Margin). The Guardband approach, outlined in Algorithm 1, augments

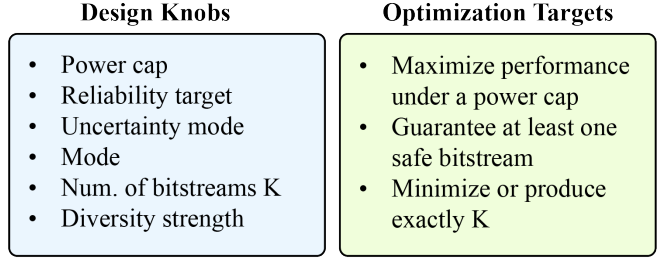


Figure 8. Capstone optimization framework.

the compiler’s power prediction with a fixed multiplicative margin. Let $\hat{P}(x)$ denote the power model’s estimate (in mW) for PnR configuration x ($graph, f_{MHz}, \Pi$). We form a conservative upper bound with guardband denoted as $U_{gb}(x)$:

$$U_{gb}(x) = (1 + \gamma)\hat{P}(x), \quad \gamma \geq 0,$$

and declare x as *safe* if $U_{gb}(x) \leq C$, where C is the user-specified power cap.

Because γ is a static user input and not learned from calibration data, this method does not provide a formal statistical coverage guarantee. Instead, it implicitly assumes that the worst-case relative *underestimation* error on future designs does not exceed γ . In practice, the guardband parameter γ can be viewed as a compact surrogate for the (unknown) aggregate error distribution across all modeling sources, including technology mismatch, PVT variation, workload mis-modeling, and abstraction errors in the energy model. Meeting the cap at runtime, therefore, requires choosing a sufficiently conservative γ (e.g., 0.15–0.30) to cover modeling bias and distribution shift. In this work, we treat γ as a user-controlled safety knob and leave systematic guardband selection policies to future work. The key advantage of this approach is its practicality: it requires no calibration dataset, is trivial to deploy, and thus forms a natural baseline for comparison.

During the post-PnR iterative pipelining loop, the compiler generates a sequence of candidate configurations $\{x_t\}$ with non-decreasing frequency $\{f_t\}$ as pipelining deepens. At each iteration t , we compute $\hat{P}(x_t)$ and $U_{gb}(x_t)$:

- **Safety anchor.** We maintain an anchor candidate using a large guardband γ_{anchor} . Whenever $U_{gb}^{anchor}(x_t) \leq C$, we update the anchor to x_t . The anchor is the configuration we rely on to satisfy the cap if deployed alone, provided the modeling error is within γ_{anchor} .
- **Speculative set.** In parallel, we track up to $K - 1$ speculative candidates using a less conservative guardband $\gamma_{spec} < \gamma_{anchor}$ to admit higher frequencies while still enforcing $U_{gb}^{spec}(x_t) \leq C$. We add a small diversity penalty in a lightweight feature space (e.g., interconnect stream count, total PE ports used, rounded frequency) so the returned set of K bitstreams does not contain near-duplicates. This reduces correlated error modes and

empirically improves the probability of meeting the “at least one is safe” objective.

- **Stopping rule.** We continue pipelining while the best speculative bound remains under the cap and while more critical paths can be broken. When $U_{\text{gb}}^{\text{spec}}(x_t) > C$, we stop and return the anchor and the top speculative designs for a total of K bitstreams.

Because both \hat{P} and the guardband scale with frequency, U_{gb} naturally tightens or loosens as f changes without additional tuning. Users control the trade-off via design knobs: γ_{anchor} , γ_{spec} , K , the power cap C , and a diversity strength.

Algorithm 1 Guardband Planner

Require: Power cap cap ; output limit K ; guardbands $\gamma_{\text{anc}}, \gamma_{\text{spec}}$; diversity weight λ ; min frequency step Δf ; power model $P(\cdot)$; features $\phi(\cdot)$

Ensure: Up to K bitstreams, including one safe anchor

```

1: Initialize:  $candidates \leftarrow \emptyset$ 
2:  $anchor \leftarrow \perp$ 
3:  $f_{\text{prev}} \leftarrow 0$ 
4: function SCORE( $x$ ) ▷ Frequency with diversity penalty
5:   return  $f(x) - \lambda \sum_{y \in candidates} \frac{\phi(x) \cdot \phi(y)}{\|\phi(x)\| \|\phi(y)\|}$ 
6: for each pipelined design  $x$  in increasing frequency do
7:   if  $f(x) < f_{\text{prev}} + \Delta f$  then
8:     continue
9:    $\mu \leftarrow P(x)$ 
10:   $U_{\text{anc}} \leftarrow (1 + \gamma_{\text{anc}})\mu$ 
11:   $U_{\text{spec}} \leftarrow (1 + \gamma_{\text{spec}})\mu$ 
12:  if  $U_{\text{anc}} \leq cap$  then
13:     $anchor \leftarrow x$ 
14:  if  $U_{\text{spec}} \leq cap$  then
15:    if  $|candidates| < K - 1$  then
16:      add  $x$  to  $candidates$ 
17:    else
18:       $y \leftarrow$  lowest-score element in  $candidates$ 
19:      if  $Score(x) > Score(y)$  then
20:        replace  $y$  with  $x$ 
21:    else
22:      break
23:   $f_{\text{prev}} \leftarrow f(x)$ 
24:  $S \leftarrow \{anchor\} \cup$  top elements of  $candidates$ 
25: return  $S$ 

```

Since Capstone I does not provide a formal guarantee that a safe bitstream will be returned, it can be naturally augmented with a simple runtime failure mechanism. Modern commercial SoCs already expose on-chip power meters that periodically write aggregate power measurements into memory-mapped registers. If a deployed bitstream is detected to exceed the power cap, the system can trigger coarse-grained architectural throttling (e.g., aggressive DVFS reduction or

frequency capping) to promptly bring power back under budget [2, 31, 40, 60]. In effect, the guardband width trades off steady-state performance against the expected rate of such runtime throttling events: wider guardbands reduce the likelihood of triggering throttling, while narrower guardbands increase performance but rely more heavily on the fallback mechanism. Exploring the full design space of such runtime mechanisms is orthogonal to this work.

Capstone II: Conformal-Envelope Planner (Learned Safety Margin). While the Guardband approach is trivial to deploy when calibration data is scarce, a conformal envelope can tighten conservatism without sacrificing guarantees by leveraging calibration data to learn a finite-sample, distribution-free error margin [8, 9, 20, 45, 77]. If the kernel being power-analyzed is very similar to the examples in the PTPX-estimated training set, then the power estimate is likely to be accurate. Therefore, we can apply a smaller guardband around it. If the kernel is very different, with high levels of composition to produce an energy estimate, then it is likely to be less accurate, and we need a larger guardband. Algorithm 2 outlines our conformal approach.

As before, let $\hat{P}(x)$ denote the power model’s estimate (in mW) for PnR configuration x ($graph, f_{\text{MHz}}, \Pi$). From a calibration set of tuples

$$\mathcal{D}_{\text{cal}} = \{(x_i, P_i^{\text{PTPX}}, \hat{P}_i, g_i)\}_{i=1}^n,$$

we form one-sided nonconformity scores

$$s_i = \max(0, P_i^{\text{PTPX}} - \hat{P}_i),$$

that quantify underestimation (the failure mode that can violate a power cap). For a user-chosen miscoverage level $\alpha \in (0, 1)$ and (optionally) a grouping key g (e.g., group by kernel), we compute the empirical upper quantile

$$q_\alpha(g) = \text{Quantile}_{1-\alpha}(\{s_i : g_i = g\})$$

$$q_\alpha(\text{global}) = \text{Quantile}_{1-\alpha}(\{s_i\}_{i=1}^n),$$

and define the conformal upper bound

$$U_{\text{conf}}(x) = \hat{P}(x) + \rho(f_{\text{MHz}}) \cdot q_\alpha(g(x)),$$

$$\rho(f) = \max\left(1, \frac{f}{f_{\text{ref}}}\right),$$

where $\rho(\cdot)$ optionally scales the margin with frequency relative to a reference f_{ref} (e.g., 100 MHz) to handle near-linear growth of residuals with f . We use $q_\alpha(g)$ when sufficient calibration points exist for group g , otherwise we fall back to $q_\alpha(\text{global})$. Under the standard exchangeability assumption between calibration and future points, the one-sided conformal bound satisfies the probability

$$\Pr\left(P^{\text{true}}(x) \leq U_{\text{conf}}(x)\right) \geq 1 - \alpha$$

If $U_{\text{conf}}(x) \leq C$, the anchor design is guaranteed to meet the power cap at runtime with confidence at least $1 - \alpha$. If the user requests a set-level confidence $1 - \epsilon$ to guarantee that at least one returned bitstream is under the power cap, we map (α, K) to ϵ via a union bound ($K\alpha \leq \epsilon$) without independence assumptions, or via a product bound $\prod_{i=1}^K (1 - \alpha_i) \geq 1 - \epsilon$ if independence is determined to be reasonable.

The planner logic and selection mechanics are otherwise identical to the Guardband case (Sec . III-B) regarding the definitions of a safety anchor, speculative set, and stopping rule. We simply substitute U_{conf} for U_{gb} .

Algorithm 2 Conformal-Envelope Planner

Require: Conformal levels $\alpha_{\text{anc}}, \alpha_{\text{spec}}$; calibration data $\{(P_j^{\text{PTPX}}, \hat{P}_j, g_j, f_j)\}$; optional frequency scaling flag s_f ;

1: (all other inputs as in Algorithm 1)

Ensure: Up to K bitstreams with conformal power guarantees

2: **Offline calibration:**

3: **for** each calibration sample j **do**

4: $r_j \leftarrow P_j^{\text{PTPX}} - \hat{P}_j$ ▷ Model residual

5: **if** $s_f = 1$ **then**

6: $r_j \leftarrow r_j / \max(1, f_j/100)$

7: **for** each group g (or one global group) **do**

8: $q_{\text{anc}}(g) \leftarrow (1 - \alpha_{\text{anc}})$ quantile of $\{r_j : g_j = g\}$

9: $q_{\text{spec}}(g) \leftarrow (1 - \alpha_{\text{spec}})$ quantile of $\{r_j : g_j = g\}$

10: **function** UPPERBOUND(μ, f, g, mode)

11: **if** $\text{mode} = \text{anchor}$ **then**

12: $q \leftarrow q_{\text{anc}}(g)$

13: **else**

14: $q \leftarrow q_{\text{spec}}(g)$

15: $\text{scale} \leftarrow \max(1, f/100)$ if $s_f = 1$ else 1

16: **return** $\mu + \text{scale} \cdot q$

17: **Online selection:**

18: Run Algorithm 1, replacing the power checks as follows:

19: **for** each pipelined design x **do**

20: $\mu \leftarrow P(x)$

21: $g \leftarrow$ group label for x (or global)

22: $U_{\text{anc}} \leftarrow \text{UPPERBOUND}(\mu, f(x), g, \text{anchor})$

23: $U_{\text{spec}} \leftarrow \text{UPPERBOUND}(\mu, f(x), g, \text{spec})$ ▷ All other steps identical to Algorithm 1

Capstone III: Guarantees with Bounded Inaccuracy.

While the Guardband and Conformal-Envelope planners of Capstone I and Capstone II, respectively, can yield a high probability of meeting a user-specified power cap when tuned conservatively, they provide only a probabilistic guarantee at a chosen confidence level. This follows from our earlier observation that power estimation, especially at higher levels of the computing stack, inevitably incurs some inaccuracy. Conformal approaches, in particular, build their confidence from

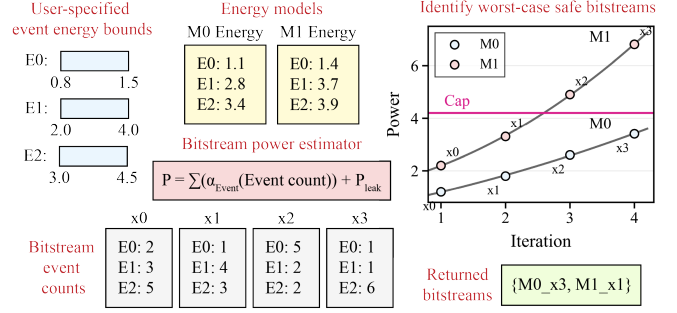


Figure 9. Variations in energy modeling can lead to different feasible bitstreams being selected under the power cap.

the assumption that their training set correlates with ground truth. In contrast, we also consider the scenario of desiring a full guarantee: the PnR configuration bitstreams returned by the compiler should include at least one that meets the power cap in real silicon deployment, even under scenarios that *differ significantly* from conditions observed in training data.

Whereas Capstone I aggregates all model uncertainty into a single scalar guardband γ without explicitly modeling any error ranges, Capstone III instead decomposes and bounds each source of error at the energy-event level. Dealing with unbounded error and providing any kind of guarantee is infeasible. However, if the user is willing to provide an exhaustive specification of error bounds on the energy model (i.e., specifying an individual error bound on the cost of each compiler-level energy event), then it becomes possible to exhaustively analyze the set of all scenarios of model inaccuracy.

Accordingly, we define a third planner mode in which Capstone performs an exhaustive error search within user-specified bounds. Concretely, we take the energy model with an annotated set of user-specified error bounds and instantiate multiple energy models that sweep across the cross product of possible evaluations in discretized steps. The errors may reflect differences in modeling strategy, technology, process variation, and other factors at user discretion. For example, Figure 9 depicts a base model M_0 and a second model M_1 where the cost estimates for events $E0, E1, E2$ are scaled, each within user-specified error bounds, to other discrete event costs. For each model M_i , the final power estimate produces a different curve relative to the power cap. Across the exhaustive set of all possible power models, we simply select for each one the single bitstream that falls underneath the cap while minimizing remaining headroom. Capstone outputs the union of these bitstreams as a set, eliminating duplicates of the same configuration, with optional further coalescing. If the user ensures that at least one model M_i in this family captures the true discrepancy between ground-truth power and the compiler’s base model, then the bitstream selected for that M_i is guaranteed to meet the power cap at runtime.

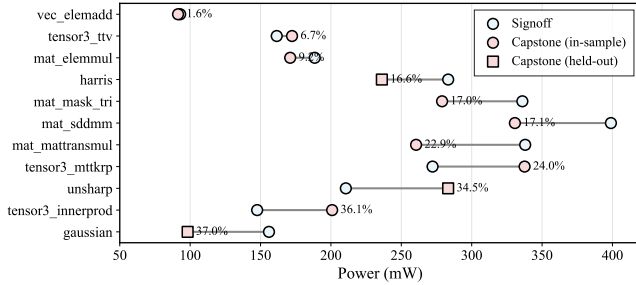


Figure 10. Signoff vs Capstone model power at 100 MHz.

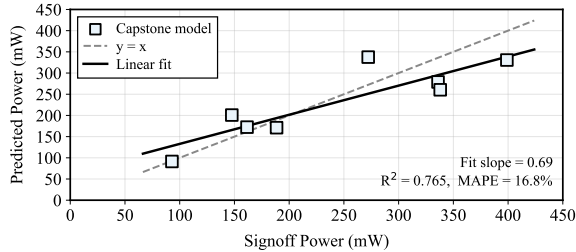


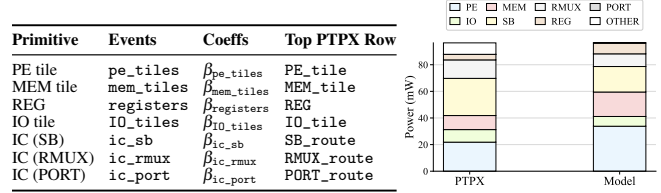
Figure 11. Gate-level vs Capstone model bias. Each point indicates a kernel. Capstone model: $R^2 = 0.765$, slope = 0.69, MAPE = 16.8%.

IV. EVALUATION

Our experiments target a 32×16 CGRA fabric in Intel 16nm technology generated by Garnet [65], consisting of PE, MEM, and I/O tiles connected through a programmable routing interconnect. Interconnect segments support optional pipeline registers that can be inserted by the compiler during the post-PnR iterative pipelining loop. We hold the fabric parameters (array dimensions, switchbox topology, and routing widths) fixed across all experiments. We evaluate a suite of fundamental dense and sparse kernels used by Cascade. Dense kernels are generated using Halide [56] and Clockwork [24] and represented as CoreIR [11] dataflow graphs, while sparse kernels are generated by Custard and translated to the SAM [22] dataflow graph representation.

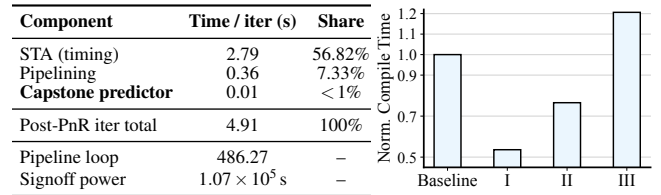
We use a Cascade-derived [48] compiler flow for scheduling, placement, and routing, augmented with the Capstone’s energy model and three controller modes (Section III). All experiments share the same ASIC toolchain (Cadence and Synopsys). Cascade’s STA reports the achievable frequency at each post-PnR pipelining iteration, while Capstone’s energy model runs inline in the loop and requires no waveform simulation or activity extraction.

Because we do not have access to a physical CGRA platform, we emulate per-kernel reconfiguration by taking the final post-PnR application graph produced by Cascade and translating it to RTL, which we then run through a full ASIC flow (synthesis, PnR, and signoff). We use the final post-pipelining graph because it contains the maximum number of compiler-inserted pipeline registers, increasing the number of exercised interconnect and register primitives available for learning power coefficients from hierarchical reports. Finally,



(a) Mapping of events to PTPX rows. (b) Power breakdown.

Figure 12. Learned primitive coefficients and model breakdown. Panel (a) shows the induced groupings from compiler events to PRIMETIME PX primitives. Panel (b) compares the Capstone model-predicted and PTPX signoff breakdown for `vec-elemadd`.



(a) Run time breakdown. (b) Norm. compile time.

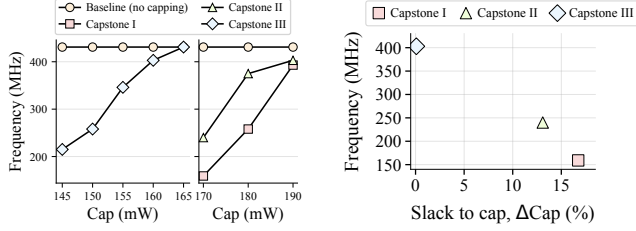
Figure 13. Run time impact of Capstone for `tensor3-ttv`.

we perform signoff post-PnR power analysis with parasitics and gate-level switching activity from compiled testbenches to generate the PTPX reports used to train Capstone’s energy model. This approach does not compromise the validity of our conclusions as all kernels share the same calibrated primitive models and testbench methodology, and only the routed application graph differs across the kernels.

A. Energy Model Accuracy, Interpretability, and Overhead

We evaluate Capstone’s hierarchical learned energy model along three axes that are required for compile-time power-capped optimization: (i) *predictive accuracy* versus signoff gate-level power, (ii) *interpretability* of the learned event-to-hardware decomposition, and (iii) *run time overhead* when used inside the post-PnR optimization loop.

Figure 10 compares Capstone’s predicted power against PTPX for each benchmark at a fixed operating point. Each dumbbell reports the signoff PTPX total and the Capstone model estimate, with the annotated label indicating percentage error relative to signoff. Across kernels, Capstone tracks signoff close enough to preserve the ordering of kernels by power. This is important for inner-loop use as the controller relies not only on absolute accuracy, but also on stable ranking between nearby configurations when deciding which PnR solution is most cap-efficient. Figure 11 summarizes the same experiment as a calibration plot of predicted power versus PTPX, with a $y=x$ reference line. Capstone predictions lie close to the diagonal, achieving high correlation ($R^2 = 0.765$) and low error (MAPE = 16.8%), indicating that a single model generalizes across diverse kernels without any kernel-specific tuning. The fitted line has slope 0.69 with intercept



(a) Max. achievable frequency. (b) Slack-Frequency Tradeoff.

Figure 14. Capstone controller evaluation for `tensor3-ttv`. (a) Maximum frequency as a function of the cap. (b) Slack-to-cap vs frequency at $C=170$ mW (Capstone III), $C=160$ mW (Capstone II).

Controller	Success rate	Med. ΔCap (%)	95th ΔCap (%)	Avg. norm. freq.	K
Baseline	0%	–	–	1.0	4
Capstone I	100%	25.99	26.04	0.46	4
Capstone II	100%	23.14	23.29	0.65	4
Capstone III	100%	16.45	19.93	1.0	90

Figure 15. Aggregate controller metrics across all (kernel, cap) pairs.

64.12 mW, indicating a systematic scaling bias with a modest additive offset rather than purely random scatter.

Beyond matching total power, we evaluate whether the learned model induces a meaningful mapping from compiler-visible events to gate-level power contributors. Figure 12(a) reports the learned primitive-level coefficients and the dominant PTPX rows selected for each compiler event group. The learned mapping aligns with architectural intuition. PE-related events concentrate on PE tile instances, MEM events align with memory structures, and interconnect events map to routing and register resources. This indicates that the model is not merely fitting totals, but is discovering a consistent *structural* correspondence between compiler activity and physical hardware power. Figure 12(b) further validates this by comparing Capstone’s primitive-level breakdown against PTPX aggregates for a representative kernel. The breakdowns agree closely, with small residuals expected from cross-kernel calibration, indicating that Capstone’s sum-of-products estimator preserves the physical split across PE, MEM, and interconnect power. This decomposition also provides a diagnostic advantage. When predictions deviate, the mismatch can often be attributed to a specific primitive bucket (e.g., PE, MEM, or interconnect), rather than appearing only as an undifferentiated total-power error. Overall, Figure 12 demonstrates that Capstone achieves both *accuracy* and *interpretability*, which is essential for trustworthy compile-time optimization.

Finally, we measure the overhead of using Capstone’s predictor within Cascade’s post-PnR optimization loop. Figure 13(a) reports a per-iteration run time breakdown for a representative kernel. STA dominates iteration time (56.82%), while Cascade’s pipelining contributes 7.33%. The Capstone predictor adds <1% of the per-iteration run time, making its cost negligible relative to the existing compilation flow while providing an $10^7 \times$ speedup over signoff power estimation.

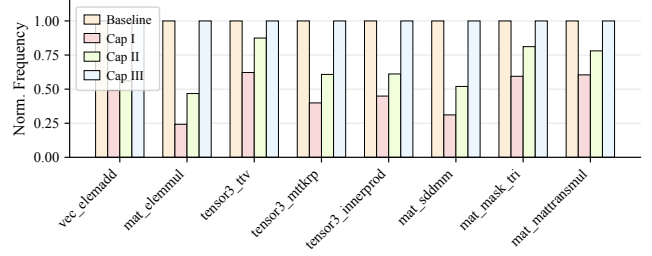


Figure 16. Normalized frequency by kernel, comparing no capping to Capstone I, II, and III controllers under fixed, per-kernel caps.

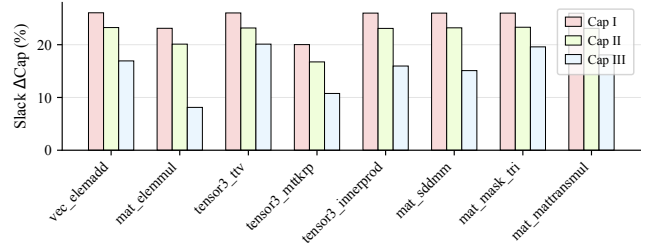


Figure 17. Slack to cap by kernel, comparing a no-capping baseline to Capstone I, II, and III controllers under fixed, per-kernel caps.

B. Compiler-Level Power-Aware Controllers

We evaluate Capstone’s three compile-time controllers: Capstone I (Guardband), Capstone II (Conformal Envelope), and Capstone III (Bounded Inaccuracy). All three modes search the same post-PnR pipelining space and they differ only in how they account for energy-model uncertainty when selecting cap-feasible solutions. We use $\gamma_{\text{spec}}=0.30$ and $\gamma_{\text{anchor}}=0.45$ for Capstone I, and $\alpha_{\text{anchor}}=0.005$ and $\alpha_{\text{spec}}=0.05$ for Capstone II, which provide stable operation near the cap. Capstone III spans the combined error space of I and II and is therefore the most aggressive controller.

We report four metrics. *Success* indicates whether the hard cap is met under signoff, and *Bitstreams K* is the number of returned PnR configurations. *Slack to cap* quantifies remaining headroom. Letting C be the cap (mW) and P the configuration’s true power, we define

$$\Delta\text{Cap} \triangleq \frac{C - P}{C} \times 100\%,$$

so feasibility requires $\Delta\text{Cap} \geq 0$, with larger values indicating more unused headroom. Finally, we report *normalized frequency*, defined as achieved frequency divided by the baseline (no-capping) frequency for the same (kernel, C) pair.

To build intuition, Figure 14 studies controller behavior on a single representative kernel. Figure 14(a) plots maximum achievable frequency versus the power cap C . Unlike the no-capping baseline, all three Capstone modes track the constraint. Capstone I is most conservative, Capstone II is intermediate, and Capstone III achieves the highest frequency. We report the most aggressive Capstone III bitstream selected from its candidate set, which matches the baseline because

TABLE III. COMPARISONS WITH PRIOR CGRA COMPILERS AT A TARGET POWER CAP.

Compiler	Tech.	Fabric	Workload	Cap (mW)	Freq. (MHz)	Power (mW)	ΔCap (%)	Success
RipTide	22FFL	6×6	FFT	365	50/25/12.5	0.24/0.12/0.06	99.93/99.97/99.98	Y/Y/Y
Snafu	22FFL	6×6	FFT	365	50/25/12.5	0.54/0.27/0.135	99.85/99.93/99.97	Y/Y/Y
UE-CGRA	28nm	8×8	FFT	365	750/325/162.5	14/7/3.5	96.16/98.1/99.04	Y/Y/Y
Plasticine	28nm	–	Inner Prod.	225	280/140/70	18900/9450/4725	-8300/-4100/-2000	Y/Y/Y
Cascade	12nm	32×16	Inner Prod.	225	481/240.5/120.25	189.1/94.6/47.3	15.96/7.98/3.99	N/N/N
Capstone I	16nm	32×16	Inner Prod.	225	216/108/54	166.5/83.3/41.6	26/13/6.5	Y/Y/Y
Capstone II	16nm	32×16	Inner Prod.	225	294/147/73.5	173/86.5/43.3	23.1/11.6/5.8	Y/Y/Y
Capstone III	16nm	32×16	Inner Prod.	225	481/240.5/120.25	189.1/94.6/47.3	15.96/7.98/3.99	Y/Y/Y
Cascade	12nm	32×16	SDDMM	365	479/239.5/119.75	310.2/115.1/57.55	15.1/7.6/3.8	Y/Y/Y
Capstone I	16nm	32×16	SDDMM	365	149/74.5/37.25	270.9/135.5/67.7	26/13/6.5	Y/Y/Y
Capstone II	16nm	32×16	SDDMM	365	249/124.5/62.25	281.1/140.6/70.3	23.2/11.6/5.8	Y/Y/Y
Capstone III	16nm	32×16	SDDMM	365	479/239.5/119.75	310.2/115.1/57.55	15.1/7.6/3.8	Y/Y/Y

maximal pipelining remains under the cap. Figure 14(b) plots slack-to-cap ($\Delta\text{Cap} \geq 0$) versus selected frequency, illustrating the safety-performance tradeoff. Capstone I caps a conservative upper bound and therefore stops pipelining earliest, leaving the most headroom. Capstone II tightens slack while retaining robustness. Capstone III caps only the prediction, pipelines further, and operates closest to the cap.

Cross-workload results confirm these trends. Figure 16 shows that Capstone III achieves the highest normalized frequency across nearly all kernels, with Capstone II capturing much of the gain. Complementarily, Figure 17 shows the same ordering in conservativeness: Capstone I leaves the most slack, Capstone II reduces slack substantially, and Capstone III operates nearest the cap while remaining feasible.

Figure 15 summarizes feasibility and headroom over all (kernel, cap) pairs. The baseline achieves 0% success because it does not enforce power constraints, whereas all Capstone modes achieve 100% success by construction under the assumed conservative parameters for Capstone I/II. Median and tail slack quantify the intended spectrum from conservative (Capstone I) to balanced (Capstone II) to aggressive yet cap-safe (Capstone III). For each controller, we evaluate both anchor and speculative candidates and report the highest-frequency design that remains feasible under the corresponding cap bound. On average, speculation provides a $4.1\times$ frequency uplift while reducing headroom by 24.6% relative to the anchor (lower ΔCap).

We note that although Capstone III achieves the highest performance, its large number of bitstreams can complicate run time deployment when K is unconstrained. In practical systems, this overhead can be mitigated by selecting a small, fixed K (as in Capstone I/II) or by falling back on architectural throttling mechanisms when necessary. Over long deployment periods, the cost of attempting a small number of candidate bitstreams amortizes away, and thus we do not study large- K run time selection further.

Finally, Figure 13(b) shows that enabling Capstone increases compile time by at most 20% relative to the baseline and in some cases reducing total compile time when early

cap detection halts pipelining, all while replacing an otherwise prohibitively expensive signoff power invocation.

C. Comparisons with State-of-the-Art CGRAs

To compare Capstone’s unique capabilities against state-of-the-art CGRA compilers, we evaluate all three optimization targets across a class of kernels with similar compute intensity. Capstone is the only approach that performs *compiler-level* power capping via a learned energy model and controller. All other existing compilers assume no power awareness, but we consider *optimistic baselines* in which architecture-level power capping is applied in the form of throttling at an even duty cycle [2, 31, 40]. We emulate this behavior using each compiler’s absolute frequency and power data without re-scaling to normalize the node (technology, fabric dimensions, etc.) to characterize these prior designs as accurately as possible. We then construct aggressive $2\times$ and $4\times$ throttle points by halving these values consecutively, corresponding to architecturally sending in data at half the rate to reduce power. This scaling is reflected in the three values (original, $2\times$, $4\times$ throttle) listed in each cell in Table III.

To study cap-aware behavior across operating regimes resembling real deployment scenarios, we evaluate multiple absolute cap settings C (mW) per kernel ($C = 365$), with only one set presented in Table III. Across all settings, Capstone is the only flow that consistently meets the cap while minimizing remaining headroom ΔCap , at the cost of generating K candidate bitstreams instead of a single design point. Other compilers may satisfy some caps only incidentally. By contrast, Capstone targets cap compliance by construction, using conservative guardbands in Capstone I/II and searching over K candidates in Capstone III to ensure at least one cap-compliant design. In some cases such as that reported, Capstone III matches the no-capping baseline because the maximally pipelined design already lies below the chosen cap.

V. CONCLUSION

Modern spatial reconfigurable accelerator compilers are power-unaware and offer no mechanism to honor system-

and component-level power budgets. We introduced Capstone, a compiler-level power-capping framework that couples a fast, automated approach to energy modeling with three power-aware compile-time controller modes: (I) guardband, (II) conformal-envelope, and (III) bounded-error. Our approach addresses activity estimation and run time bottlenecks, so that power can be evaluated on each iteration of the inner pipelining loop, with Capstone also accounting explicitly for the potential impact of modeling error. Capstone is, to our knowledge, the first approach to deliver CGRA compiler-level power capping that tunes design configurations to a specific power target while optimizing to preserve performance.

REFERENCES

- [1] E. aliagha, N. Charaf, N. K. Venkatesan, and D. Göhringer. DA-CGRA: Domain-Aware Heterogeneous Coarse-Grained Reconfigurable Architecture for the Edge. *Euromicro Conference on Digital System Design (DSD)*, Aug 2024.
- [2] J. Aragon, J. Gonzalez, and A. Gonzalez. Power-aware control speculation through selective throttling. *Int'l Symp. on High-Performance Computer Architecture (HPCA)*, Feb 2003.
- [3] Y. Cao, D. Li, Y. Zhang, Q. Tang, A. Khodaei, H. Zhang, and Z. Han. Optimal Energy Management for Multi-Microgrid Under a Transactive Energy Framework With Distributionally Robust Optimization. *IEEE Transactions on Smart Grid*, Jan 2022.
- [4] T. Chen, A. Rucker, and G. E. Suh. Execution time prediction for energy-efficient hardware accelerators. *Int'l Symp. on Microarchitecture (MICRO)*, Oct 2015.
- [5] Y. Cho and I. Yang. Data-Driven Stochastic Optimization Using Upper Confidence Bounds: Performance Guarantees and Distributional Robustness. *IEEE Conference on Decision and Control (CDC)*, Mar 2023.
- [6] M. Chu, D. Allstot, J. Huard, and K. Wong. NSGA-based parasitic-aware optimization of a 5GHz low-noise VCO. *Asia and South Pacific Design Automation Conference (ASP-DAC)*, Jan 2004.
- [7] J. Coburn, S. Ravi, and A. Raghunathan. Power emulation: a new paradigm for power estimation. *Design Automation Conf. (DAC)*, Jun 2005.
- [8] M. Cocheteux, J. Moreau, and F. Davoine. Uncertainty-Aware Online Extrinsic Calibration: A Conformal Prediction Approach. *IEEE/CVF Winter Conference on Applications of Computer Vision (WACV)*, Feb 2025.
- [9] K. M. Cohen, S. Park, O. Simeone, and S. Shamai Shitz. Calibrating AI Models for Wireless Communications via Conformal Prediction. *IEEE Transactions on Machine Learning in Communications and Networking*, Sep 2023.
- [10] C. Dai, L. Wu, and H. Wu. A Multi-Band Uncertainty Set Based Robust SCUC With Spatial and Temporal Budget Constraints. *IEEE Transactions on Power Systems*, Nov 2016.
- [11] R. Daly, L. Truong, and P. Hanrahan. Invoking and Linking Generators from Multiple Hardware Languages using CoreIR. *In Workshop on Open-Source EDA Technology (WOSET)*, Sep 2018.
- [12] D. Y. Deng and G. E. Suh. High-performance parallel accelerator for flexible and efficient run-time monitoring. *IEEE/IFIP Int'l Conference on Dependable Systems and Networks*, 2012.
- [13] C. Duan, W. Fang, L. Jiang, L. Yao, and J. Liu. Distributionally Robust Chance-Constrained Approximate AC-OPF With Wasserstein Metric. *IEEE Transactions on Power Systems*, Sep 2018.
- [14] C. Ebeling, D. C. Cronquist, and P. Franklin. RaPiD: Reconfigurable Pipelined Datapath. *Int'l Conf. on Field Programmable Logic (FPL)*, Sep 1996.
- [15] X. Fan, D. Wu, W. Cao, W. Luk, and L. Wang. Stream Processing Dual-Track CGRA for Object Inference. *IEEE Trans. on Very Large-Scale Integration Systems (TVLSI)*, Feb 2018.
- [16] M. J. Feizollahi, S. Ahmed, and M. Modarres. The Robust Redundancy Allocation Problem in Series-Parallel Systems With Budgeted Uncertainty. *IEEE Transactions on Reliability*, Mar 2014.
- [17] X. Gao, Y. Qiu, Y. Dai, W. Yin, and L. Wang. A CGRA Front-end Compiler Enabling Extraction of General Control and Dedicated Operators. *Asia and South Pacific Design Automation Conference (ASP-DAC)*, Jan 2024.
- [18] G. Gobieski, A. O. Atli, K. Mai, B. Lucia, and N. Beckmann. Snafu: An Ultra-Low-Power, Energy-Minimal CGRA-Generation Framework and Architecture. *Int'l Symp. on Computer Architecture (ISCA)*, Jun 2021.
- [19] G. Gobieski, S. Ghosh, M. Heule, T. Mowry, T. Nowatzki, N. Beckmann, and B. Lucia. RipTide: A Programmable, Energy-Minimal Dataflow Compiler and Architecture. *Int'l Symp. on Microarchitecture (MICRO)*, Oct 2022.
- [20] V. Gopakumar, A. Gray, J. Oskarsson, L. Zanisi, S. Pamela, D. Giles, M. Kusner, and M. P. Deisenroth. Uncertainty Quantification of Surrogate Models using Conformal Prediction. *arXiv preprint arXiv:2408.09881*, Aug 2024.
- [21] M. Hamzeh, A. Shrivastava, and S. Vrudhula. EPIMap: using epimorphism to map applications on CGRAs. *Design Automation Conf. (DAC)*, Jun 2012.
- [22] O. Hsu, M. Strange, R. Sharma, J. Won, K. Olukotun, J. S. Emer, M. A. Horowitz, and F. Kjølstad. The sparse abstract machine. *Int'l Conf. on Architectural Support for Programming Languages and Operating Systems (ASPLOS)*, Mar 2023.
- [23] Y. Huang, P. Jenne, O. Temam, Y. Chen, and C. Wu. Elastic CGRAs. *Int'l Symp. on Field Programmable Gate Arrays (FPGA)*, Feb 2013.
- [24] D. Huff, S. Dai, and P. Hanrahan. Clockwork: Resource-Efficient Static Scheduling for Multi-Rate Image Processing Applications on FPGAs. *Int'l Symposium on Field-Programmable Custom Computing Machines*, Jun 2021.
- [25] S. M. A. H. Jafri, O. Bag, A. Hemani, N. Farahini, K. Paul, J. Plosila, and H. Tenhunen. Energy-aware coarse-grained reconfigurable architectures using dynamically reconfigurable isolation cells. *Int'l Symp. on Quality Electronic Design (ISQED)*, Mar 2013.
- [26] X. Jiao, A. Rahimi, B. Narayanaswamy, H. Fatemi, J. P. de Gyvez, and R. K. Gupta. Supervised learning based model for predicting variability-induced timing errors. *IEEE International New Circuits and Systems Conference (NEWCAS)*, Jun 2015.
- [27] M. Karunarathne, A. K. Mohite, T. Mitra, and L.-S. Peh. HyCUBE: A CGRA with Reconfigurable Single-cycle Multi-hop Interconnect. *Design Automation Conf. (DAC)*, Jun 2017.
- [28] C. Kim, M. Chung, Y. Cho, M. Konijnenburg, S. Ryu, and J. Kim. ULP-SRP: Ultra low power Samsung Reconfigurable Processor for biomedical applications. *International Conference on Field-Programmable Technology (FPT)*, Dec 2012.
- [29] D. Kim, A. Izraelevitz, C. Celio, H. Kim, B. Zimmer, Y. Lee, J. Bachrach, and K. Asanović. Strober: fast and accurate sample-based energy simulation for arbitrary RTL. *SIGARCH Comput. Archit. News*, Jun 2016.
- [30] D. Kim, J. Zhao, J. Bachrach, and K. Asanović. Simmani: Runtime Power Modeling for Arbitrary RTL with Automatic Signal Selection. *Int'l Symp. on Microarchitecture (MICRO)*, Oct 2019.
- [31] Y. Kim, L. K. John, I. Paul, S. Manne, and M. Schulte. Performance boosting under reliability and power constraints. *Int'l Conf. on Computer-Aided Design (ICCAD)*, Nov 2013.

- [32] T. Kojima, B. Adhi, C. Cortes, Y. Tan, and K. Sano. An Architecture-Independent CGRA Compiler enabling OpenMP Applications. *IEEE International Parallel and Distributed Processing Symposium Workshops (IPDPSW)*, May 2022.
- [33] G. Korol, M. Jordan, M. Brandalero, M. B. Rutzig, and A. C. S. Beck. Power-Aware Phase Oriented Reconfigurable Architecture. *IEEE International Conference on Electronics, Circuits and Systems (ICECS)*, Nov 2019.
- [34] G. Korol, M. Jordan, R. S. Silva, M. M. Pereira, M. Brandalero, M. B. Rutzig, and A. C. S. Beck. A Runtime Power-Aware Phase Predictor for CGRAs. *IEEE International Conference on ReConfigurable Computing and FPGAs (ReConFig)*, Dec 2019.
- [35] K. Koul, J. Melchert, K. Sreedhar, L. Truong, G. Nyengele, K. Zhang, Q. Liu, J. Setter, P.-H. Chen, Y. Mei, M. Strange, R. Daly, C. Donovan, A. Carsello, T. Kong, K. Feng, D. Huff, A. Nayak, R. Setaluri, J. Thomas, N. Bhagdikar, D. Durst, Z. Myers, N. Tsiskaridze, S. Richardson, R. Bahr, K. Fatahalian, P. Hanrahan, C. Barrett, M. Horowitz, C. Torng, F. Kjolstad, and P. Raina. AHA: An Agile Approach to the Design of Coarse-Grained Reconfigurable Accelerators and Compilers. *IEEE Trans. on Embedded Computing Systems (TECS)*, Jan 2023.
- [36] A. K. A. Kumar, S. Al-Salamin, H. Amrouch, and A. Gerstlauer. Machine Learning-Based Microarchitecture-Level Power Modeling of CPUs. *IEEE Transactions on Computers*, Apr 2023.
- [37] A. K. A. Kumar and A. Gerstlauer. Learning-Based CPU Power Modeling. *ACM/IEEE 1st Workshop on Machine Learning for CAD (MLCAD)*, 2019.
- [38] T. A. Le, Q.-T. Vien, H. X. Nguyen, D. W. K. Ng, and R. Schober. Robust Chance-Constrained Optimization for Power-Efficient and Secure SWIPT Systems. *IEEE Transactions on Green Communications and Networking*, Sep 2017.
- [39] D. Lee and A. Gerstlauer. Learning-Based, Fine-Grain Power Modeling of System-Level Hardware IPs. *ACM Transactions on Design Automation of Electronic Systems (TODAES)*, Feb 2018.
- [40] S.-W. Lee and J.-L. Gaudiot. Throttling-Based Resource Management in High Performance Multithreaded Architectures. *IEEE Transactions on Computers*, Sep 2006.
- [41] B. Li, Y. Tan, A.-G. Wu, and G.-R. Duan. A Distributionally Robust Optimization Based Method for Stochastic Model Predictive Control. *IEEE Transactions on Automatic Control*, Nov 2022.
- [42] S. Li, J. H. Ahn, R. D. Strong, J. B. Brockman, D. M. Tullsen, and N. P. Jouppi. The McPAT Framework for Multicore and Manycore Architectures: Simultaneously Modeling Power, Area, and Timing. *ACM Trans. on Architecture and Code Optimization (TACO)*, 10(1):5:1-5:29, Apr 2013.
- [43] Z. Lin, J. Zhao, S. Sinha, and W. Zhang. HL-Pow: A Learning-Based Power Modeling Framework for High-Level Synthesis. *IEEE Asia and South Pacific Design Automation Conference (ASP-DAC)*, Jan 2020.
- [44] S. Liu, R. N. Pittman, A. Forin, and J.-L. Gaudiot. Achieving energy efficiency through runtime partial reconfiguration on reconfigurable systems. *ACM Trans. Embed. Comput. Syst.*, Mar 2013.
- [45] C. Lu, Y. Yu, S. P. Karimireddy, M. Jordan, and R. Raskar. Federated Conformal Predictors for Distributed Uncertainty Quantification. *Proceedings of the 40th International Conference on Machine Learning (ICML)*, PMLR 202:22942-22964, Jul 2023.
- [46] Y. Luo, C. Tan, N. B. Agostini, A. Li, A. Tumeo, N. Dave, and T. Geng. ML-CGRA: An Integrated Compilation Framework to Enable Efficient Machine Learning Acceleration on CGRAs. *IEEE International Parallel and Distributed Processing Symposium Workshops (IPDPSW)*, Jul 2023.
- [47] B. Mei, S. Vernalde, D. Verkest, H. De Man, and R. Lauwereins. DRESC: a retargetable compiler for coarse-grained reconfigurable architectures. *IEEE International Conference on Field-Programmable Technology*, Dec 2002.
- [48] J. Melchert, Y. Mei, K. Koul, Q. Liu, M. Horowitz, and P. Raina. Cascade: An Application Pipelining Toolkit for Coarse-Grained Reconfigurable Arrays. *IEEE Trans. on Computer-Aided Design of Integrated Circuits and Systems (TCAD)*, Oct 2024.
- [49] S. M. Nabavinejad, S. Reda, and M. Ebrahimi. BatchSizer: Power-Performance Trade-off for DNN Inference. *Proceedings of the 26th Asia and South Pacific Design Automation Conference (ASPDAC)*, Jan 2021.
- [50] S. M. Nabavinejad, S. Reda, and M. Ebrahimi. Coordinated Batching and DVFS for DNN Inference on GPU Accelerators. *IEEE Transactions on Parallel and Distributed Systems*, Jan 2022.
- [51] D. V. C. d. Nascimento, K. Georgiou, K. I. Eder, and S. Xavier-de Souza. Evaluating the Effects of Reducing Voltage Margins for Energy-Efficient Operation of MPSoCs. *IEEE Embedded Systems Letters*, Mar 2024.
- [52] Y. Nasser, J. Lorandell, J.-C. Prévotet, and M. H elard. RTL to Transistor Level Power Modeling and Estimation Techniques for FPGA and ASIC: A Survey. *IEEE Transactions on Computer-Aided Design of Integrated Circuits and Systems*, Jun 2021.
- [53] M. Perry, J. Xu, E. Huang, and C.-H. Chen. Robust Sampling Budget Allocation Under Deep Uncertainty. *IEEE Transactions on Systems, Man, and Cybernetics: Systems*, Oct 2022.
- [54] R. Prabhakar, Y. Zhang, D. Koeplinger, M. Feldman, T. Zhao, S. Hadjis, A. Pedram, C. Kozyrakis, and K. Olukotun. Plasticine: A Reconfigurable Architecture For Parallel Patterns. *Int'l Symp. on Computer Architecture (ISCA)*, Jun 2017.
- [55] K. Prabhu, R. M. Radway, J. Yu, K. Bartolone, M. Giordano, F. Peddinghaus, Y. Urman, W.-S. Khwa, Y.-D. Chih, M.-F. Chang, S. Mitra, and P. Raina. MINOTAUR: An Edge Transformer Inference and Training Accelerator with 12 MBytes On-Chip Resistive RAM and Fine-Grained Spatiotemporal Power Gating. *IEEE Symposium on VLSI Technology and Circuits (VLSI Technology and Circuits)*, Jun 2024.
- [56] J. Ragan-Kelley, C. Barnes, A. Adams, S. Paris, F. Durand, and S. Amarasinghe. Halide: A language and compiler for optimizing parallelism, locality, and recomputation in image processing pipelines. *ACM Sigplan Not.* 48, 6, Jun 2013.
- [57] A. Rahimi, L. Benini, and R. K. Gupta. Hierarchically focused guardbanding: an adaptive approach to mitigate PVT variations and aging. *Design, Automation, and Test in Europe (DATE)*, Mar 2013.
- [58] A. Rahimi, L. Benini, and R. K. Gupta. Application-Adaptive Guardbanding to Mitigate Static and Dynamic Variability. *IEEE Transactions on Computers*, Sep 2014.
- [59] H. V. Ranjitha, S. Hiremath, and S. G. Langadi. RTL Power Estimation: Early Design Cycle Approach for SoC Power Sign-Off. *IEEE International Conference on Recent Trends in Electronics, Information and Communication Technology (RTEICT)*, May 2018.
- [60] V. J. Reddi, M. S. Gupta, G. Holloway, G.-Y. Wei, M. D. Smith, and D. Brooks. Voltage Emergency Prediction: Using Signatures to Reduce Operating Margins. *Int'l Symp. on High-Performance Computer Architecture (HPCA)*, Feb 2009.
- [61] P. K. Rout, D. P. Acharya, and G. Panda. A Multiobjective Optimization Based Fast and Robust Design Methodology for Low Power and Low Phase Noise Current Starved VCO. *IEEE Transactions on Semiconductor Manufacturing*, Feb 2014.
- [62] Y. S. Shao, B. Reagen, G.-Y. Wei, and D. Brooks. Aladdin: A Pre-RTL, Power-Performance Accelerator Simulator Enabling Large Design Space Exploration of Customized Architectures. *Int'l Symp. on Computer Architecture (ISCA)*, Jun 2014.
- [63] H. Singh, M.-H. Lee, G. Lu, N. Bagherzadeh, F. J. Kurdahi, and E. M. C. Filho. MorphoSys: An Integrated Reconfigurable System for Data-Parallel and Computation-Intensive Applications. *IEEE Transactions on Computers*, May 2000.

- [64] A. Srivastava, T. Kachru, and D. Sylvester. Low-Power-Design Space Exploration Considering Process Variation Using Robust Optimization. *IEEE Transactions on Computer-Aided Design of Integrated Circuits and Systems*, Jan 2007.
- [65] Stanford AHA! Agile Hardware Center. garnet: Next generation CGRA generator. GitHub repository, 2019.
- [66] J. Sun, C. Talarico, P. Gupta, and J. Roveda. A New Uncertainty Budgeting-Based Method for Robust Analog/Mixed-Signal Design. *ACM Transactions on Design Automation of Electronic Systems (TODAES)*, Nov 2015.
- [67] T. Tang, S. Li, L. Nai, N. Jouppi, and Y. Xie. NeuroMeter: An Integrated Power, Area, and Timing Modeling Framework for Machine Learning Accelerators Industry Track Paper. *Int'l Symp. on High-Performance Computer Architecture (HPCA)*, Feb 2021.
- [68] H. Tann, S. Hashemi, R. I. Bahar, and S. Reda. Runtime configurable deep neural networks for energy-accuracy trade-off. *IEEE/ACM/IFIP Int'l Conference on Hardware/Software Codesign and System Synthesis (CODES)*, Oct 2016.
- [69] C. Torng, P. Pan, Y. Ou, C. Tan, and C. Batten. Ultra-Elastic CGRAs for Irregular Loop Specialization. *Int'l Symp. on High-Performance Computer Architecture (HPCA)*, Feb 2021.
- [70] A. Vasilyev, N. Bhagdikar, A. Pedram, S. Richardson, S. Kvatinsky, and M. Horowitz. Evaluating programmable architectures for imaging and vision applications. *Int'l Symp. on Microarchitecture (MICRO)*, Oct 2016.
- [71] J. Wang, K. Li, J. Chen, R. Shi, L. Chen, and W. Chen. Power Prediction of RTL-Level Circuits by Using Machine Learning. *IEEE International Symposium of Electronics Design Automation (ISED)*, May 2023.
- [72] W. Wei, F. Liu, and S. Mei. Distributionally Robust Co-Optimization of Energy and Reserve Dispatch. *IEEE Transactions on Sustainable Energy*, Jan 2016.
- [73] C. Xu, F. X. Lin, Y. Wang, and L. Zhong. Automated OS-level Device Runtime Power Management. *Int'l Conf. on Architectural Support for Programming Languages and Operating Systems (ASPLOS)*, Mar 2015.
- [74] S. Xu and B. C. Schafer. Approximate Reconfigurable Hardware Accelerator: Adapting the Micro-Architecture to Dynamic Workloads. *Int'l Conf. on Computer Design (ICCD)*, Nov 2017.
- [75] J. Yang, L. Ma, K. Zhao, Y. Cai, and T.-F. Ngai. Early stage real-time SoC power estimation using RTL instrumentation. *Asia and South Pacific Design Automation Conference (ASPDAC)*, Jan 2015.
- [76] L. Yang, Y. Xu, H. Sun, and W. Wu. Tractable Convex Approximations for Distributionally Robust Joint Chance-Constrained Optimal Power Flow Under Uncertainty. *IEEE Transactions on Power Systems*, May 2022.
- [77] C. Yeh, N. Christianson, A. Wu, A. Wierman, and Y. Yue. End-to-End Conformal Calibration for Optimization Under Uncertainty. *arXiv preprint arXiv:2409.20534*, Sep 2024.
- [78] T. Yu, O. Ragheb, S. Wicklund, and J. Anderson. MLIR-to-CGRA: A Versatile MLIR-Based Compiler Framework for CGRAs. *International Conference on Application-specific Systems, Architectures and Processors (ASAP)*, Jul 2024.
- [79] H. Zhang and P. Li. Chance Constrained Programming for Optimal Power Flow Under Uncertainty. *IEEE Transactions on Power Systems*, Nov 2011.
- [80] Y. Zhang, H. Ren, and B. Khailany. GRANNITE: Graph Neural Network Inference for Transferable Power Estimation. *Design Automation Conf. (DAC)*, Jul 2020.
- [81] Y. Zhang, N. Zhang, T. Zhao, M. Vilim, M. Shahbaz, and K. Olukotun. SARA: Scaling a Reconfigurable Dataflow Accelerator. *Int'l Symp. on Computer Architecture (ISCA)*, Jun 2021.
- [82] Z. Zhang, S. Lin, M. Dedeoglu, K. Ding, and J. Zhang. Data-driven Distributionally Robust Optimization for Edge Intelligence. *IEEE Conference on Computer Communications*, Jul 2020.
- [83] Z. Zhao, W. Sheng, Q. Wang, W. Yin, P. Ye, J. Li, and Z. Mao. Towards Higher Performance and Robust Compilation for CGRA Modulo Scheduling. *IEEE Transactions on Parallel and Distributed Systems*, Apr 2020.
- [84] Y. Zhou, H. Ren, Y. Zhang, B. Keller, B. Khailany, and Z. Zhang. PRIMAL: Power Inference using Machine Learning. *Design Automation Conf. (DAC)*, Jun 2019.
- [85] D. Zoni, L. Cremona, and W. Fornaciari. PowerProbe: Run-time power modeling through automatic RTL instrumentation. *Design, Automation, and Test in Europe (DATE)*, Mar 2018.
- [86] D. Zoni, L. Cremona, and W. Fornaciari. All-Digital Energy-Constrained Controller for General-Purpose Accelerators and CPUs. *IEEE Embedded Systems Letters*, Mar 2020.
- [87] D. Zoni, A. Galimberti, and W. Fornaciari. A Survey on Run-time Power Monitors at the Edge. *ACM Comput. Surv.*, Jul 2023.